Enhanced surface and interface magnetism of bcc Ni overlayers on Fe(001)

J. I. Lee,* Soon C. Hong,† and A. J. Freeman
Department of Physics and Astronomy, Northwestern University, Evanston, Illinois 60208

C. L. Fu
Metals and Ceramics Division, Oak Ridge National Laboratory, Oak Ridge, Tennessee 37831
(Received 31 January 1992)

The surface and interface magnetism of metastable bcc Ni as an overlayer on Fe(001)—originally synthesized by Heinrich *et al.*—is investigated using the highly precise total-energy full-potential linearized augmented plane-wave method. Two systems—a monolayer (1Ni/Fe) and a bilayer (2Ni/Fe) coverage on Fe(001)—are investigated and compared. The Ni-Fe interlayer spacings are found to be relaxed downward by 2.5% and 4% for 1Ni/Fe and 2Ni/Fe, respectively. The effect of the Ni-Fe hybridization on the electronic and magnetic properties is examined. In both overlayer systems the magnetic moments at the interface Ni and Fe sites are enhanced relative to their corresponding bulk values. The magnetic moment ($0.69\mu_B$) of the surface Ni atom of 2Ni/Fe is found to be reduced from that ($0.86\mu_B$) of the surface Ni atom on 1Ni/Fe. A manifestation of the moment enhancement at the interface Fe site is a positive contribution to the hyperfine field from the valence electrons.

I. INTRODUCTION

Recently developed sophisticated synthesis techniques now permit the fabrication of a variety of artificial materials (thin films, sandwiches, and modulated structures) and hold out the promise of making materials with desired properties of specification.[1] Successful applications of these techniques include the synthesizing of metastable states of transition metals on favorable substrates: thus, metastable bcc Co has been synthesized[2] on GaAs and metastable bcc Ni has been grown[3] on Fe by molecular-beam epitaxy methods. These achievements have raised theoretical questions on the correlation between structure and magnetism. Thus, their bulk properties have been investigated by several groups,[4,5] using highly precise band methods based on the local (spin) density-functional formalism.[6]

These metastable transition-metal phases have also provided new surfaces to be investigated. The surface magnetism of bcc Co for the (001) (Ref. 7) and (110) (Ref. 8) surfaces has already been investigated by means of the full potential linearized augmented plane-wave (FLAPW) method,[9,10] and these results have increased our knowledge about the surface magnetism in transition metals. A scaling of the enhancement of the magnetic moment in bcc Co for the (001) and (110) surfaces was found to be similar to the case for the same Fe[11,12] surfaces. Other physical properties are also similar for these two transition metals, except that bcc Co has a shorter screening length for spin density than does Fe.

To examine both surface and interface effects, we have calculated the electronic and magnetic structure of a monolayer and bilayer of bcc Ni on Fe(001). In Sec. II we briefly describe our model and method. The calculated results for each of the systems, monolayer and bilayer bcc Ni on Fe, are presented in parallel and are discussed in Sec. III. A summary is given in Sec. IV.

II. METHOD

We have adopted the slab model to investigate the surface and interface magnetism of bcc Ni as an overlayer on Fe(001). To examine the surface and interface effects concurrently, we have taken two slab systems: a monolayer of Ni attached to each side of a five-layer Fe(001) film, and bilayer bcc Ni on each side of the same Fe film. The bulk value of the lattice constant is used for the Fe substrate. The interlayer distance between Fe and Ni is determined from total-energy calculations. The Ni-Ni distance in bilayer bcc Ni is assumed to be the same as in fcc Ni.

We solve the Kohn-Sham local-density-functional equations self-consistently by using the FLAPW method. In the FLAPW method[9,10] no shape approximations are made to the potential or the charge density in solving Poisson's equation; the general potential is rigorously taken into account in all parts of space. The charge density and potential inside the MT spheres are expanded into lattice harmonics with angular momentum up to $l=8$. The wave functions inside the MT sphere are also constructed by the same set of lattice harmonics. The explicit form of von Barth and Hedin for the exchange-correlation potential[13] is employed for this spin-polarized study.

A fully relativistic calculation is made for the core electrons, whereas the valence electrons are treated semirelativistically,[14] i.e., ignoring spin-orbit coupling. For the monolayer and bilayer Ni on Fe slabs, approximately 2×240 and 2×310 LAPW basis functions are used, respectively, for each of the 21 k points in the irreducible wedge of the two-dimensional Brillouin zone. Convergence is assumed when the rms differences between the input and output total charge and spin densities are less than $3\times10^{-4}e/(\text{a.u.})^3$.

III. RESULTS

This section presents and compares results obtained for both the monolayer and bilayer bcc Ni on Fe(001). We denote the monolayer and bilayer Ni on Fe(001) by 1Ni/Fe and 2Ni/Fe, respectively.

A. Structural properties: Total-energy studies

Since strong hybridization between the Fe-*d* and Ni-*d* bands is expected, the bond length between the Fe and Ni atoms should affect the electronic structure and magnetism of the 1Ni/Fe and 2Ni/Fe systems. To determine the effect of relaxation, we allowed the interlayer spacing between Ni-Fe to be relaxed, while the atomic distances between Ni-Ni and Fe-Fe were kept to their corresponding bulk values.

Figure 1 shows the total-energy difference curve as a function of Ni-Fe interlayer spacing for 1Ni/Fe. The solid circles represent our calculated data points, which are fitted to a parabola (solid line). The total-energy minimum is found at 2.39 a.u., which corresponds to a 2.5% downward relaxation compared to the unrelaxed Ni-Fe interlayer distance (taken as the average of the bulk Fe-Fe and Ni-Ni bond lengths). This 2.5% downward relaxation is much smaller than those found in nonmagnetic/magnetic overlayer systems, e.g., Al/Fe(001)[15] and Fe/W(110),[16] because of the magnetic pressure effect which tends to expand the interatomic distances.

The total-energy difference curve for 2Ni/Fe (cf. Fig. 2) shows the total energy to be a minimum at the interlayer spacing of 2.34 a.u. (corresponding to a 4% downward relaxation). In the case of Fe/W(110), adding an overlayer reduces the downward relaxation from 9.5% to 4.0%. However, in these systems the additional Ni layer induces an enhancement of the downward relaxation rather than its reduction. The reason is that the additional Ni layer reduces the magnetic moment of Ni and Fe atoms at the interface and so reduces the magnetic pressure.

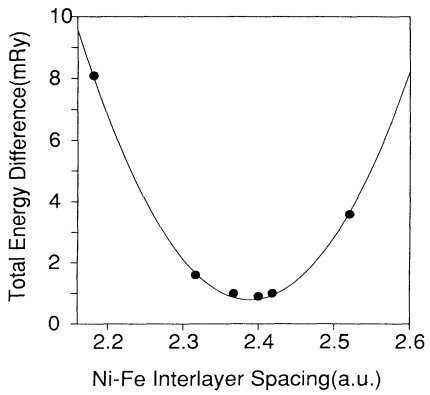

FIG. 1. Total-energy difference for the 1Ni/Fe as a function of the Ni/Fe interlayer spacing.

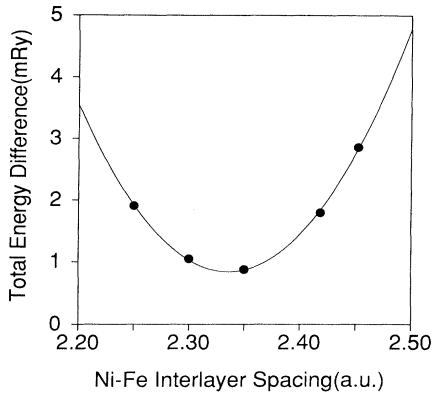

FIG. 2. Total-energy difference for the 2Ni/Fe as a function of the Ni-Fe interlayer spacing.

B. Charge densities and work functions

The charge densities, the central quantities in local density theory, are given in Figs. 3(a) and 3(b) for the relaxed 1Ni/Fe and 2Ni/Fe, respectively. These contours clearly show that the charge-density distribution at the metal-vacuum interface tends to smooth out the discontinuous nature of the surface by a spatial redistribution of *s*, *p*-like electrons in the surface layer. Despite the corrugation of the surface atoms, the charge-density contours become almost structureless about 1 Å above the surface-vacuum boundary.

In order to describe the charge configuration quantitatively, we decompose the majority- and minority-spin electrons inside the MT spheres by angular momentum and by layer (cf. Table I). It is seen that the interface effect on the charge configuration is confined to the interface and the charge configuration of the subinterface Fe is almost the same as that of the center Fe. The number of electrons of the interface Fe for both of 1Ni/Fe and 2Ni/Fe increases by about 0.1, compared to the corresponding unrelaxed Ni/Fe systems and becomes almost the same as that of the inner Fe layers as the Ni-Fe interface gets relaxed. The Ni surface atom of 1Ni/Fe has about 0.1 electrons more than that of 2Ni/Fe; recall that the FLAPW calculations for the clean Fe(001) surface found that the surface Fe atom has about 0.2 electrons less than the inner Fe layers,[11] indicating that the electrons transfer from Ni to Fe sites.

The electrons spilled out into the vacuum region determine, in a delicate way, the electrostatic surface dipole layer and thus the work function. The calculated work functions are 4.91 eV and 5.07 eV for spin-polarized 1Ni/Fe and 2Ni/Fe, respectively. The antibonding states of majority spin get filled with the expense of the bonding states of minority spin as the magnetic moment increases. As discussed in the Fe/Cu(001) system,[17] it may be concluded here also that the larger work function of 2Ni/Fe compared to 1Ni/Fe is principally due to the smaller magnetic moment of the surface Ni in 2Ni/Fe and that magnetism would affect electronic properties.

TABLE I. Work function (in eV), layer-by-layer magnetic moment (in μ_B) and l-decomposed majority (↑) and minority (↓) spin charges (in electrons) inside the MT sphere for monolayer bcc Ni (1Ni/Fe) and bilayer bcc Ni (2Ni/Fe) on Fe(001). Total represents the sum of majority- and minority-spin electrons.

			l decomposition of charge				Magnetic	Work
			s	p	d	Total	moment	function
1Ni/Fe	Ni(S)	(↑)	0.19	0.11	4.52	4.83	0.86	4.91
		(↓)	0.20	0.11	3.65	3.97		
		total	0.39	0.22	8.18	8.80		
	Fe(S-1)	(↑)	0.17	0.16	4.31	4.66	2.65	
		(↓)	0.17	0.17	1.66	2.01		
		total	0.34	0.33	5.97	6.67		
	Fe(S-2)	(↑)	0.17	0.15	4.27	4.57	2.44	
		(↓)	0.17	0.17	1.78	2.13		
		total	0.34	0.32	6.05	6.70		
	Fe(C)	(↑)	0.17	0.15	4.22	4.55	2.42	
		(↓)	0.17	0.17	1.78	2.13		
		total	0.34	0.32	6.00	6.68		
2Ni/Fe	Ni(S)	(↑)	0.16	0.08	4.44	4.69	0.69	5.07
		(↓)	0.17	0.09	3.74	4.00		
		total	0.33	0.17	8.18	8.69		
	Ni(S-1)	(↑)	0.20	0.17	4.43	4.81	0.69	
		(↓)	0.21	0.18	3.72	4.12		
		total	0.41	0.35	8.15	8.93		
	Fe(S-2)	(↑)	0.18	0.16	4.29	4.65	2.59	
		(↓)	0.17	0.17	1.70	2.06		
		total	0.35	0.33	5.99	6.71		
	Fe(S-3)	(↑)	0.17	0.15	4.21	4.55	2.40	
		(↑)	0.17	0.17	1.79	2.14		
		total	0.34	0.32	6.00	6.69		
	Fe(C)	(↑)	0.17	0.15	4.20	4.53	2.38	
		(↓)	0.17	0.17	1.80	2.15		
		total	0.34	0.32	6.00	6.68		

C. Spin densities and magnetic moments

Contour plots of the self-consistent spin densities on the (110) plane for relaxed 1Ni/Fe and 2Ni/Fe are given in Figs. 4(a) and 4(b), respectively. As in other surface magnetism studies of ferromagnetic transition metals, the regions of strong positive polarization of the localized d electrons are separated by regions of negative polarization of the delocalized s,p electrons. The large eruption of spin-density contours at the surfaces of both systems indicates a large enhancement of magnetic moments at their surfaces. For 1Ni/Fe(001), the surface Ni magnetic moment is enhanced to $0.86\mu_B$ [$\sim 26\%$ larger compared to that for the fcc Ni(001) surface, $0.68\mu_B$ (Ref. 9)]. This large magnetic-moment enhancement can be attributed to the interfacial Fe-Ni hybridization, i.e., the larger Fe moment induces an additional magnetic polarization at the interfacial Ni sites. Indeed, the magnetic moment of the surface Ni layer in 2Ni/Fe(001) decreases drastically to $0.69\mu_B$, almost identical to that at the fcc Ni(001) surface.

In addition to the moment enhancements at the Ni site, one of the most remarkable features found at the bcc Ni/Fe(001) interface is the enhancement of the interfacial Fe magnetic moment to $2.65\mu_B$, which lies between the magnetic moments of the surface ($2.98\mu_B$) and the subsurface Fe layers at the clean bcc Fe(001) surface. Furthermore, a comparison between the interface Fe moments in 1Ni/Fe and 2Ni/Fe (the difference between them is only $0.06\mu_B$) shows that the interface moment enhancement is not due to surface effects, but is an intrinsic property of the bcc Ni/Fe(001) interface. As also found from the Fe(001) clean surface, the surface and interface effects induce a long-range magnetic perturbation in the interior Fe layers, i.e., our FLAPW results for the magnetic moments going from the interface Fe layer to the center Fe layer of the five-layer Fe slabs are (in μ_B) 2.65 (2.59), 2.44 (2.40), and 2.42 (2.38) for 1Ni/Fe (2Ni/Fe), respectively. The magnetic moments of the Fe center layer ($2.42\mu_B$ for 1Ni/Fe and $2.38\mu_B$ for 2Ni/Fe), however, are still somewhat larger than that of the calculated bulk values, which indicate that the five-layer Fe is not thick enough to reproduce the bulk value of the magnetic moments. Note that the layer-by-layer magnetic moments, unlike the number of electrons, have no Friedel-type oscillations for 1Ni/Fe(001).

D. Hyperfine fields

As is well known, knowledge of the electron spin density at the nucleus is essential for the interpretation of hyperfine interaction measurements, which provide valu-

able information about the local magnetic structure and character of the electronic-spin polarization. Table II presents a layer-by-layer breakdown of the contact part of the hyperfine field, H_c, for the 1Ni/Fe and 2Ni/Fe systems. The decomposition into contributions from core and conduction electrons reveals the large negative core polarization expected from the exchange interaction with the magnetic moment of the localized $3d$ electrons. This contribution from the core electrons is again found to scale very precisely with the local magnetic moment for each of the Ni overlayers and Fe underlayers (cf. Table II).

We find, from Table II, that the contributions from the conduction electrons is negative in all cases except at the interface Fe layers. This fact is interesting if we recall previous FLAPW calculations, which also gave positive contributions from the conduction electrons at the ferromagnetic transition metal surfaces.[7–9,11,12] A positive

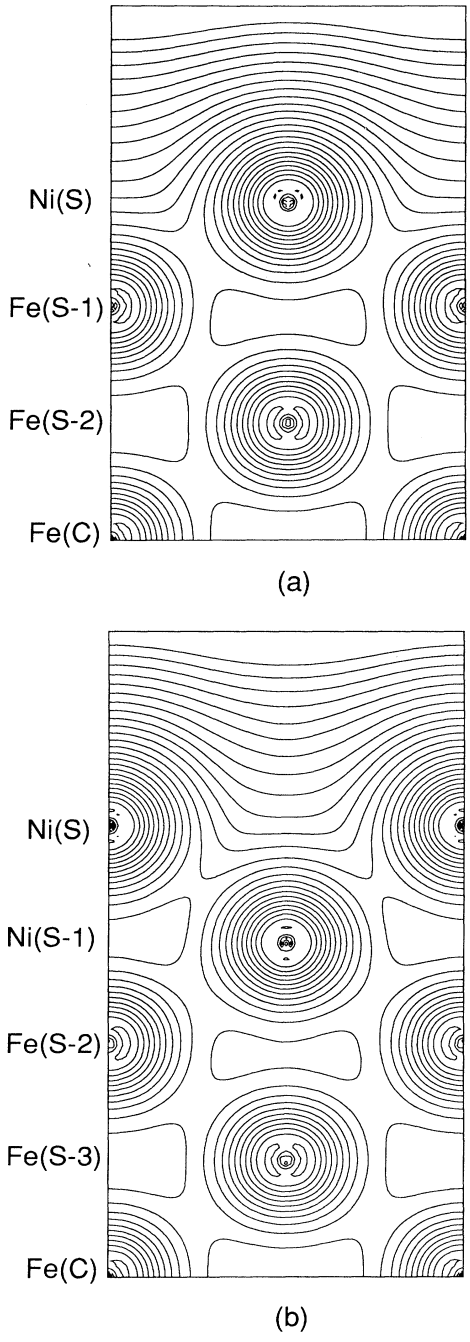

FIG. 3. Valence electronic charge density for (a) 1Ni/Fe(001) and (b) 2Ni/Fe(001) in units of $1\times10^{-3}e/(\text{a.u.})^3$ on the (110) planes. Subsequent contour lines differ by a factor of $\sqrt{2}$.

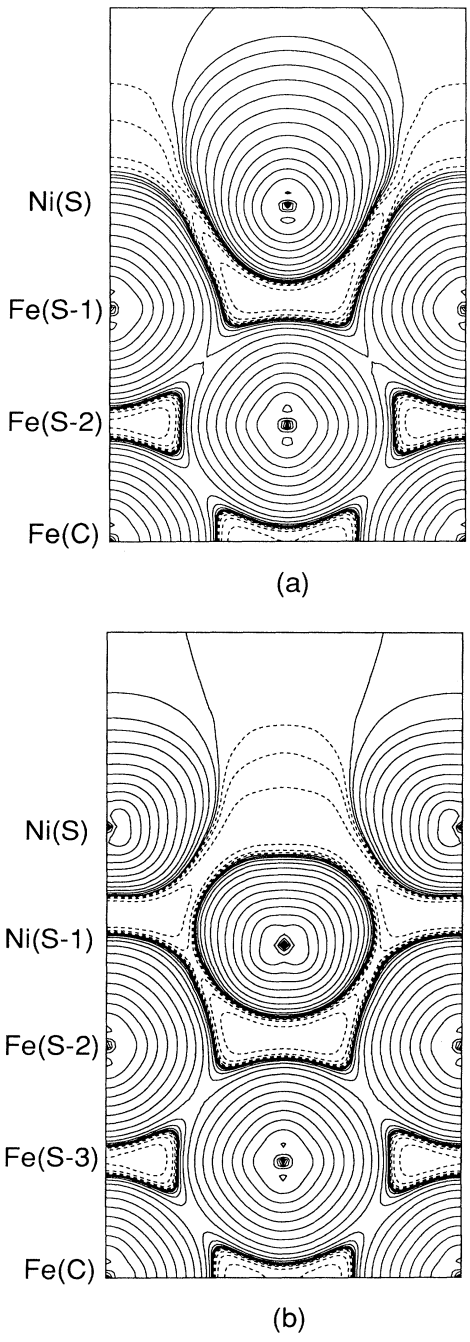

FIG. 4. Spin density for (a) 1Ni/Fe(001) and (b) 2Ni/Fe(001) in units of $1\times10^{-4}e/(\text{a.u.})^3$ on the (110) planes. Subsequent contour lines differ by a factor of 2.

TABLE II. Magnetic contact hyperfine fields (in kG) broken down into core and conduction electron contributions. The last column shows the ratio of the core contact contribution and the magnetic moment (cf. Table I) in the corresponding MT sphere (in kG/μ_B).

		Core	Conduction	Total	Core/M
1Ni/Fe	Ni(S)	−126	−109	−235	−147
	Fe(S-1)	−365	+48	−317	−138
	Fe(S-2)	−336	−28	−365	−138
	Fe(C)	−334	−38	−371	−138
2Ni/e	Ni(S)	−106	−49	−154	−153
	Ni(S-1)	−105	−111	−216	−152
	Fe(S-2)	−357	+47	−310	−138
	Fe(S-3)	−334	−49	−383	−138
	Fe(C)	−331	−32	−362	−139

H_c contribution from the conduction electrons implies that the localized d moment causes a direct polarization (i.e., atomic-like) of the s,p-like conduction electrons. At the ferromagnetic transition metal surfaces, the mechanism behind the direct polarization of the valence electrons is due to the reduced symmetry and lower coordination number (i.e., a more atomic-like environment).

Interestingly, for both the monolayer and bilayer coverage of Ni on Fe(001), the conduction electron (CE) contribution to H_c at Ni nuclei is negative (same sign as that of core contribution) at the surface and interface Ni sites. This implies that the polarization effect due to the relatively large magnetic moment at the interface Fe site on the s,p electrons of the Ni overlayers overrides the localization effect at the surface (which causes a direct atomic-like polarization of the CE).

E. Density of states and single-particle energy spectra

We now discuss the layer-by-layer DOS (LDOS) and the calculated energy-band structures of 1Ni/Fe and 2Ni/Fe. Figures 5 and 6 show the LDOS for the 1Ni/Fe

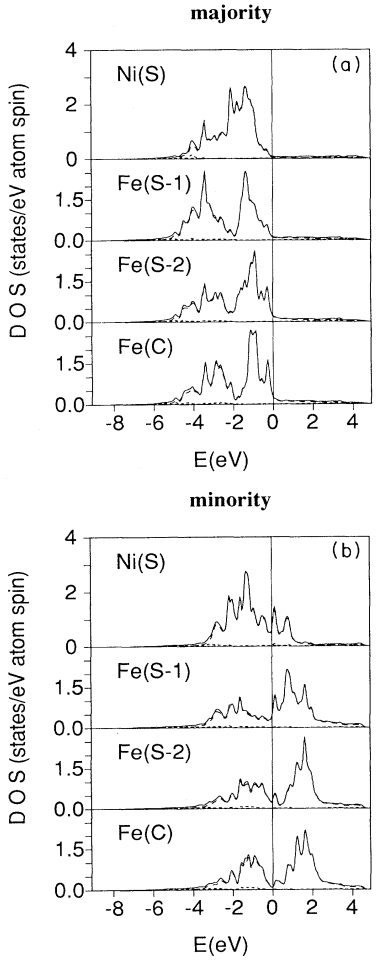

FIG. 5. Layer-by-layer partial density of states for 1Ni/Fe for (a) majority and (b) minority spins in states/eV spin atom. Dotted lines indicate d states and dashed lines represent s and p states.

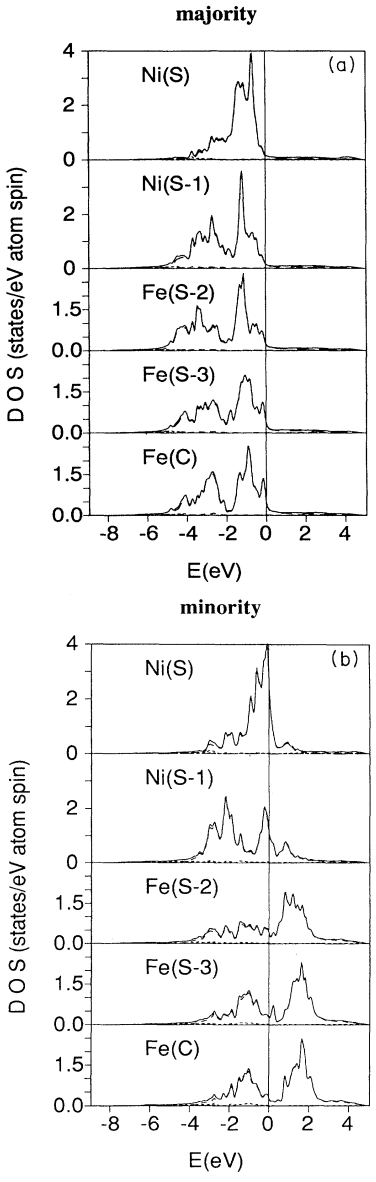

FIG. 6. Layer-by-layer partial density of states for 2Ni/Fe (as in Fig. 5).

and 2Ni/Fe, respectively. Overall, the shape of the LDOS is seen to become structureless and to narrow when going from the center layer (which has the shape of the bulk DOS with its three major peaks) to the surface layer due to the lower coordination number at the surface.

The strong hybridization between Ni and Fe bands is seen from the fact that the LDOSs for the interface Ni (the surface Ni of 1Ni/Fe and subsurface Ni of 2Ni/Fe) are much broader, compared to the surface Ni LDOS of 2Ni/Fe. The Ni-Fe hybridization on the interface Fe LDOS increases the majority-spin occupancy by shifting the LDOS features (particularly the antibonding states) to higher binding energy compared to those of the inner Fe layers (cf. Figs. 5 and 6). The strong Ni-Fe d-band interaction is also seen to cause different minority-spin LDOS shapes for the interfacial Fe layer from those of the corresponding majority-spin LDOS for the inner layers. These facts imply that the main effect of the Ni-Fe interface on the magnetization is to induce magnetic saturation at the interface Fe site through strong hybridization between the minority-spin Ni and Fe d bands. It is interesting to note that for the interface Fe minority-spin LDOS, the Fermi level is not pinned at the valley separating the bonding and antibonding states, as is the case for bulk Fe.

Consider now the calculated energy-band structure localized on the surface Ni layer. Figures 7 and 8 show the energy dispersions along the high symmetry lines for 1Ni/Fe and 2Ni/Fe, respectively; left (a) and right (b) panels correspond to majority and minority spins, respectively. The energy bands are broken down for clarity into

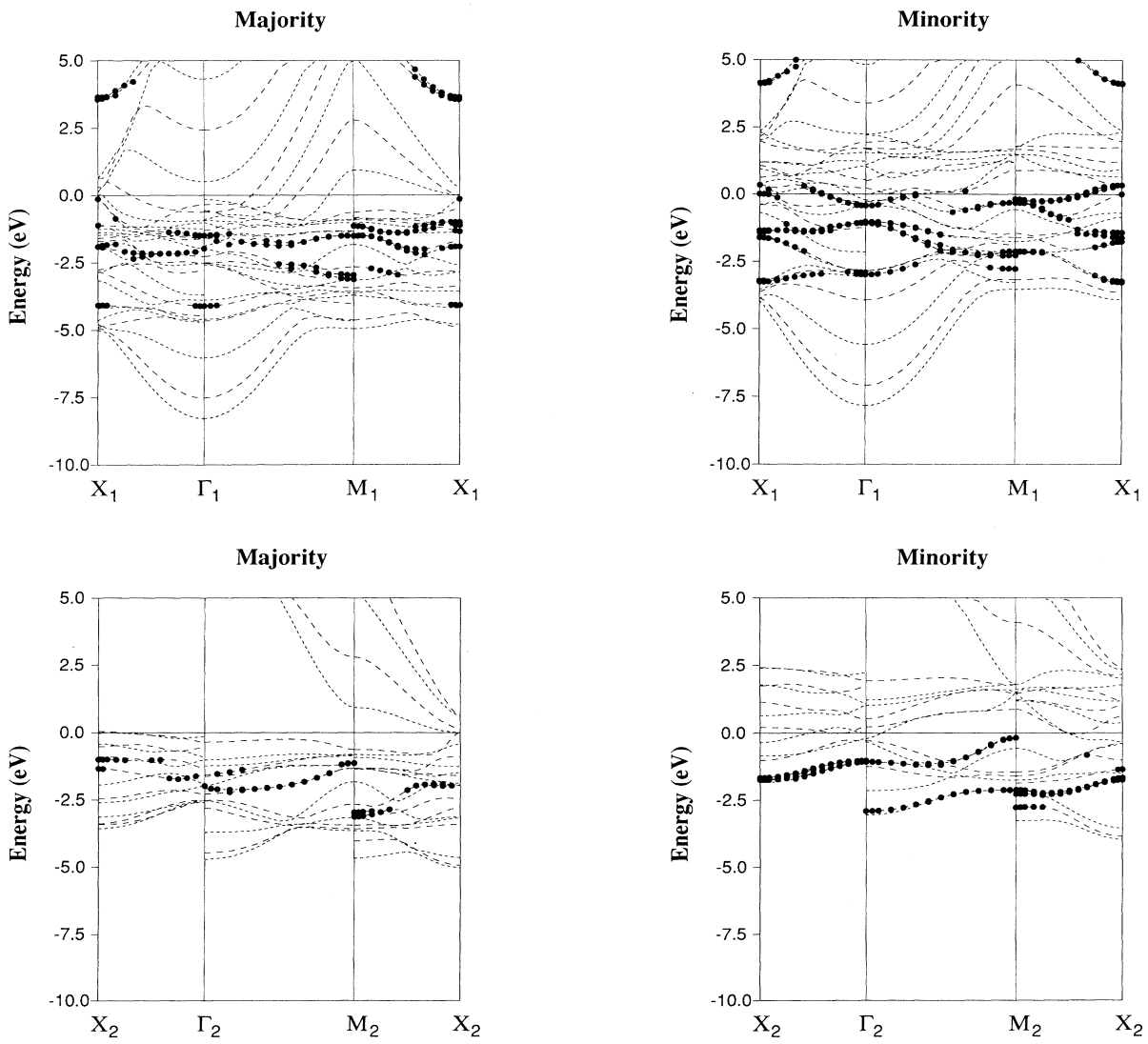

FIG. 7. Energy bands for 1Ni/Fe of majority spin and minority spin along high-symmetry directions in the 2D Brillouin zone. Top and lower panels show odd and even symmetries, respectively, with respect to the 2D rotational symmetry. Dashed and dotted lines represent odd and even parities with respect to z reflection. Solid lines indicate surface states whose wave functions have more than 50% weight within the surface layer.

their respective odd and even symmetries with respect to 2D mirror planes. The upper (lower) panel of each figure represents even (odd) symmetries. Dashed and dotted lines represent states with odd and even parities with respect to z reflection, respectively. Surface energy bands, represented by the solid circles, are defined as having more than 50% of their wave functions localized in the surface layer.

For the majority-spin band of 1Ni/Fe, we find localized surface states around the energy region 2 eV below E_F. These surface states lie in the valley between the bonding and antibonding bulk peaks of the bcc DOS and hence, they contribute to make the surface LDOS structureless. For the minority-spin case, the surface-state bands are found scattered in energy due to the hybridization of Ni-Fe bands and are shifted upwards in energy from those of the majority-spin states by ~ 1 eV, due to the magnetic exchange splitting. Furthermore, there is a considerably larger overlap of the minority-spin surface states with those of the Fe-derived bands, indicating a strong Ni-Fe minority-spin d-band interaction.

The surface states for 2Ni/Fe (cf. Fig. 8) are much less dispersive in energy and are located closer to the Fermi level than are those for 1Ni/Fe. This implies that the surface states of 1Ni/Fe originate from the Ni-Fe band hybridization.

IV. SUMMARY

The surface and interface magnetism of metastable bcc Ni as overlayers on Fe was investigated by means of the self-consistent, all-electron FLAPW method. To understand the surface and interface effects together, we have taken two systems—monolayer (1Ni/Fe) and bilayer (2Ni/Fe) bcc Ni on Fe(001). For these systems, the Ni-Fe interlayer spacing, charge and spin densities, work functions, layer-by-layer density of states, magnetic moments, and hyperfine fields were determined.

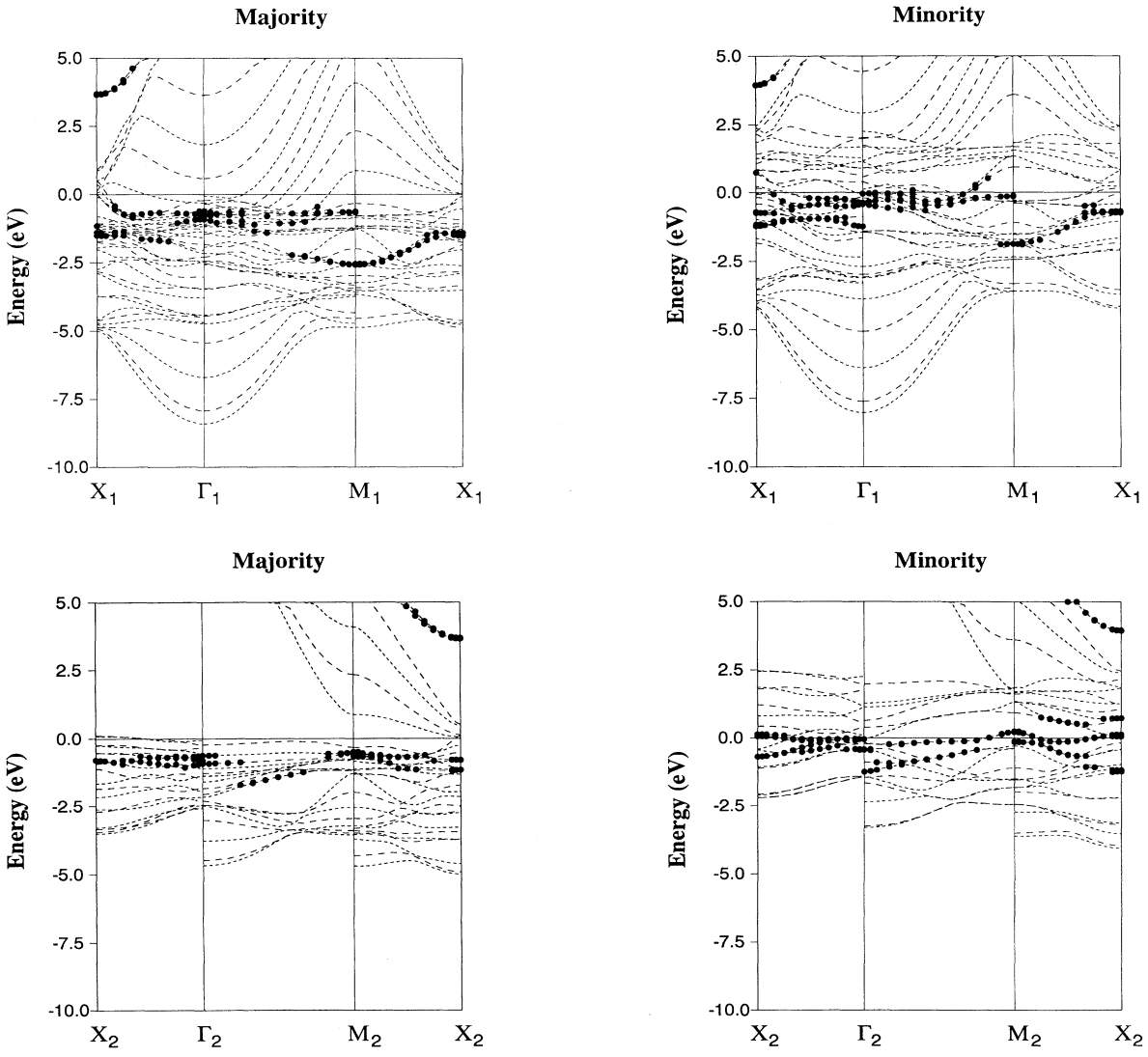

FIG. 8. Energy bands for 2Ni/Fe (as in Fig. 7).

The Ni-Fe interface is relaxed downward by 2.5% and 4% for 1Ni/Fe and 2Ni/Fe, respectively. The calculated layer-by-layer magnetic moments show that the value of the surface magnetic moment for bilayer bcc Ni on Fe($0.69\mu_B$) is smaller than that of monolayer Ni on Fe($0.86\mu_B$). The magnetic moment in the interface Fe ($2.65\mu_B$ for 1Ni/Fe and $2.59\mu_B$ for 2Ni/Fe) is not changed much by the number of Ni overlayers and is larger than that in the subsurface Fe layer in the clean bcc Fe(001) surface ($2.35\mu_B$). This also suggests strong interaction (i.e., hybridization) between the Ni and Fe atoms.

The calculated LDOS of the inner Fe layers (which has three main peaks) is typical of the LDOS of the bcc phase. The shape of the LDOS becomes structureless on going to the surface layer from the center layer, as a result of the lower coordination number at the surface. The dominant effect of the interface Fe layer is on the Ni antibonding states of minority spins.

The surface states of 1Ni/Fe for majority spin are found around 2 eV below E_F while those for minority spin are scattered in energy due to the hybridization of Ni-Fe bands. The surface states for 2Ni/Fe are much less dispersive in energy due to their localized character.

ACKNOWLEDGMENTS

We thank Dr. Ruqian Wu for helpful discussions and suggestions and for a critical review of the manuscript. Work was supported at Northwestern University by the National Science Foundation (DMR Grant No. 89-06935 and Grant No. 91-17818) and by a computing grant from its Division of Advanced Specific Computing at the National Center for Supercomputing Applications, University of Illinois. Work at Oak Ridge National Laboratory was sponsored by the Division of Materials Sciences, U.S. Department of Energy, under Contract DE-AC05-84OR21400 with Martin Marietta Energy Systems, Inc.

*Permanent address: Department of Physics, Inha University, Inchon 402-751, Korea.

†Permanent address: Department of Physics, University of Ulsan, Ulsan 680-749, Korea.

[1]A. J. Freeman, J. Magn. Mag. Mater. **15-18**, 1070 (1980).

[2]G. A. Prinz, Phys. Rev. Lett. **54**, 1051 (1985).

[3]B. Heinrich, A. S. Arrott, J. F. Cochran, C. Liu, and K. Myrtle, J. Vac. Sci. Technol. A **4**, 1376 (1986); H. Heinrich, S. T. Purcell, J. R. Dutcher, K. B. Urquhart, J. F. Cochran, and A. S. Arrott, Phys. Rev. B **38**, 12 879 (1988).

[4]V. I. Moruzzi, P. M. Marcus, K. H. Schwarz, and P. Mohn, J. Magn. Magn. Mater. **54-57**, 955 (1986); Phys. Rev. B **34**, 1784 (1986); V. I. Moruzzi, Phys. Rev. Lett. **57**, 2211 (1986).

[5]B. I. Min, T. Oguchi, and A. J. Freeman, Phys. Rev. B **33**, 7852 (1986).

[6]P. Hohenberg and W. Kohn, Phys. Rev. **136**, A864 (1964); W. Kohn and L. I. Sham, Phys. Rev. **140**, B1133 (1965); O. Gunnarson and B. I. Lundqvist, Phys. Rev. B **13**, 4274 (1976).

[7]J. I. Lee, C. L. Fu, and A. J. Freeman, J. Magn. Magn. Mater. **62**, 93 (1986).

[8]J. I. Lee, C. L. Fu, and A. J. Freeman (unpublished).

[9]E. Wimmer, A. J. Freeman, and H. Krakauer, Phys. Rev. B **30**, 3113 (1984).

[10]H. Kraukauer, A. J. Freeman, and E. Wimmer, Phys. Rev. B **28**, 610 (1983).

[11]S. Ohnishi, A. J. Freeman, and M. Weinert, Phys. Rev. B **28**, 6741 (1983).

[12]C. L. Fu and A. J. Freeman, J. Magn. Magn. Mater. **69**, L1 (1987); A. J. Freeman and C. L. Fu, J. Appl. Phys. **61**, 3356 (1987).

[13]U. von Barth and L. Hedin, J. Phys. C **5**, 1629 (1972).

[14]D. D. Koelling and B. N. Harmon, J. Phys. C **10**, 3107 (1977).

[15]S. C. Hong, J. I. Lee, and A. J. Freeman, J. Magn. Magn. Mater. **99**, L45 (1991).

[16]S. C. Hong, A. J. Freeman, and C. L. Fu, Phys. Rev. B **38**, 12 156 (1988).

[17]C. L. Fu and A. J. Freeman, Phys. Rev. B **35**, 925 (1987).